RESEARCH ARTICLE

CALIBRATION OF A THREE-DETECTOR MICROWAVE ELLIPSOMETER

[1,*]A. Moungache, [1]B. Bayard, [2]Abakar Mahamat Tahir, [3] C. Thron , [1] S. Robert, [2]F. Gambou

[1]Laboratoire Hubert Curien, UMR CNRS 5516, Université Jean Monnet, Saint-Etienne, France
[2]Université de N'Djamena, Tchad,
[3]Texas A&M University-Central Texas, Killeen Texas USA

ABSTRACT

The three-detector microwave ellipsometer working at 30 GHz frequency is an experimental bench used to characterize dielectric materials. This paper is aimed at showing the reliability of the measurement of this original bench. Thus, the latter is described first. Then, error sources and their influences on the measurement are studied. We finally show that a numerical correction used for calibration guaranties the reliability of the measurement.
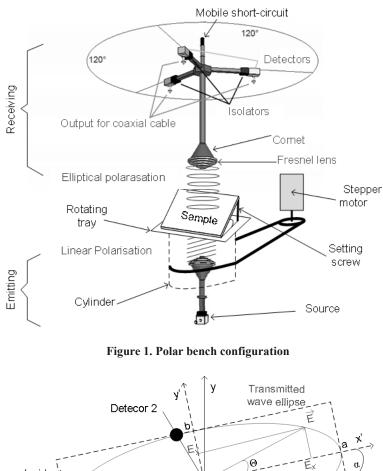
INTRODUCTION

Ellipsometry is a non-destructive characterization method of materials. It is a nonperturbing light technique that uses the state of polarization of the light upon reflection and/or transmission of an sample (El-Agez, 2010). The basic principles of ellipsometry were established since more than 60 years. Since then, many techniques have been used to develop ellipsometers for various applications such as the study of thin film surfaces or material characterization (Azzam, 1977; Aspnes, 1973; Taya, 2014; Oates, 2008; Azzam, 1987; Azzam, 1975). Initially, ellipsometry was restricted to optical frequencies (Azzam, 1977; Azzam, 1987). Optical ellipsometers contain a number of components: light sources, polarizers, analyzers, depolarizers, compensators, samples to be studied, detectors, etc. These elements are arranged in various configurations, depending on the type of measurement desired: for example, fixed or rotating polarizers may be used, in order to make reflection or transmission measurements (Taya, 2013). More recently, the concept of ellipsometry has been extended to microwave frequencies (Sagnard, 2002; Gambou, 2009). This extension was motivated by the fact that microwaves propagate better through thick and nontransparent materials. In this paper, we deal with a three-detector microwave ellipsometer operating in the range of 24-40 GHz to determine shape of the polarization ellipse for the transmitted wave through a material under test. The ellipse's characteristics may be used to determine material properties: as shown in references (Gambou *et al*., 2011; Moungache *et al*., 2015; Jarosik *et al*., 2011), the experimental device can be used to characterize the isotropy and anisotropy of a sample by determining its indices of refraction. For reliable characterization, the study of sensitivity, calibration and measurement error is necessary (Gambou, 2009; Gambou, 2011; Moungache *et al*., 2015). We have partially studied the first point in (Wehus *et al*., 2013). A complementary study of sensitivity, calibration and measurement errors is included within the scope of this article. We first show how the calibration is done, and then show how to evaluate measurement errors in order to deal with them.

MATERIALS AND METHODS

Presentation of the BENCH: Banc Polar: The configuration of this simple, free-space experimental bench is based on preliminary work described in (Raoult, 2017) to develop an ellipsometric method that uses three fixed detectors as analyzers.

---

*Corresponding author: **Moungache, A.,**
Laboratoire Hubert Curien, UMR CNRS 5516, Université Jean Monnet, Saint-Etienne, France.

The setup of the device is described in (Gambou, 2011) except the fact that the Gunn source is replaced by a Vector Network Analyzer (VNA). As shown in Figure , the device setup is made up of two fixed emitting and receiving parts aligned for transmission measurements. The sample is placed in between, and is inclined with respect to the direction of propagation so as to have oblique incidence whose φ is the incidence angle. The sample is mounted on a revolving plate actuated by a stepper motor. When rotating, the position of the sample is given by θ, (called the angular position), which is measured from the direction of the emitted linear polarization (Moungache, *et al.*, 2015). The emitting part contains a VNA source in order to produce different microwave frequencies. A rectangular waveguides is used to linearly polarize the electric field E parallel to the small side, so that only the fundamental mode TE10 propagates. The rectangular waveguide (polarizer) is connected to a circular horn antenna. The emitting process is completed with a Fresnel lens placed on the antenna, which collimates the beam to form a plane wave. The receiving part begins with a combination of a Fresnel lens and a circular horn antenna. To save the transmitted wave polarization, a circular waveguides is connected to the antenna. The transmitted wave is led to three detectors (R, A and B of the VNA) directed at 120° from each other and perpendicularly connected to the circular waveguide through portions of rectangular waveguides. The detectors are connected to a personal computer through an acquisition board to save measurement data.
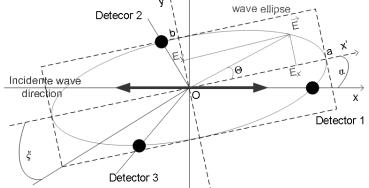

Figure 1. Polar bench configuration

Figure 2. Position of the three detectors with respect to the ellipse

Measurement principles: Generally when a linearly polarized wave interacts with a sample, it becomes elliptical (Azzam, 1996). Now, we can describe an ellipse through two angles which are the rotation α and the angular ellipticity ξ. The rotation gives the orientation of the ellipse's major axis with respect to the direction of the incident wave (Moungache *et al.*, 2015), while ξ =atan(b/a) where a and bare the semimajor and semiminor axes respectively (Figure). We define two reference frames (O, X, Y) and (O, X', Y'). The unprimed frame is fixed relative to the laboratory, and the primedrelative to the ellipse of the transmitted wave. Three points on the polarization ellipse are sufficient to determine the geometry of the ellipse. Thus three electromagnetic intensity detectors 120 °-shifted from each other and lying on the ellipse plane (Figure) are sufficient to determine the ellipse as follows. Assuming that the device is perfect (as described in reference [12]), the electromagnetic intensity in theΘ$_i$-direction is given by:

$$I_i = (a^2 + b^2) + (a^2 - b^2)\cos(2\Theta_i), \; i=1,2,3, \tag{1}$$

where Θ_1, Θ_2, Θ_3 are the angles locating the directions of the detectors, with respect to the X'

$$\Theta_1 = -\alpha, \tag{2}$$

$$\Theta_2 = -\alpha + 2\pi/3, \tag{3}$$

$$\Theta_3 = -\alpha - 2\pi/3. \tag{4}$$

Defining

$$A = a^2 + b^2, \tag{5}$$

$$B = a^2 - b^2, \tag{6}$$

substituting (5), (6) into (1), and using expressions (2-4) for Θ_i i=1,2,3 respectively leads to:

$$I_1 = A + B\cos(2\alpha), \tag{7}$$

$$I_2 = A + B\cos(-2\alpha + 4\pi/3),$$

$$I_2 = A + (B/2)\left[-\cos(2\alpha) - \sqrt{3}\sin(2\alpha)\right], \tag{8}$$

$$I_3 = A + B\cos(-2\alpha - 4\pi/3)$$

$$I_3 = A + (B/2)\left[-\cos(2\alpha) + \sqrt{3}\sin(2\alpha)\right]. \tag{9}$$

From equations (7-9), we may obtain:

$$A = (I_1 + I_2 + I_3)/3, \tag{10}$$

$$B\cos(2\alpha) = (2I_1 - I_2 - I_3)/3, \tag{11}$$

$$B\sin 2\alpha = (I_3 - I_2)/\sqrt{3}. \tag{12}$$

It follows that

$$B = \sqrt{[2I_1 - I_2 - I_3]^2/9 + [I_3 - I_2]^2/3}. \tag{13}$$

The rotation is given by

$$\tan 2\alpha = \frac{(I_3 - I_2)}{(2I_1 - I_2 - I_3)}, \tag{24}$$

and the ellipticity is

$$|e| = \frac{b}{a} = \sqrt{\frac{A-B}{A+B}}. \tag{35}$$

The angular ellipticity ξ is then given by

$$\tan\xi = |e|. \tag{46}$$

Therefore, it is possible to calculate the rotation α and the angular ellipticity ξ from the three intensity measurements.

RESULTS AND DISCUSSION

Measurement error: The principle described above at section 2.2 requires that the all components of the bench are perfect. It means that wave guides are perfectly aligned, the three branches correctly 120°- shifted from each other, etc. But in practice, measurements are tainted with various errors which may or may not be correctable. Errors may be classified as follows (González, 2010; Moffat, 1988; Taylor, 1982):
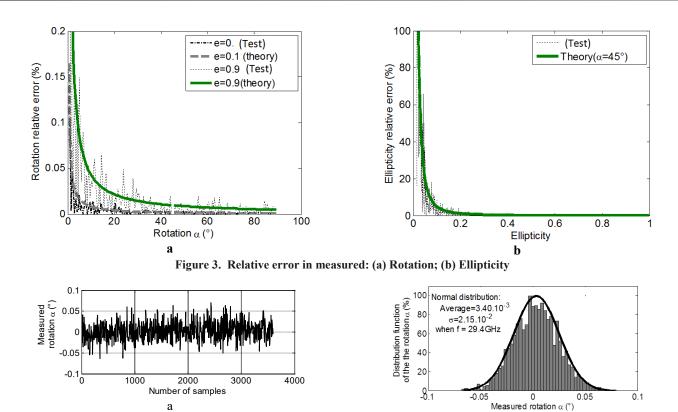
Figure 3. Relative error in measured: (a) Rotation; (b) Ellipticity

Figure 4. Influence of stepper motor vibration on the measurement. (a) Rotation α when only the stepper motor is on, but no motion of the cylinder. (b) Distribution function of the rotation α
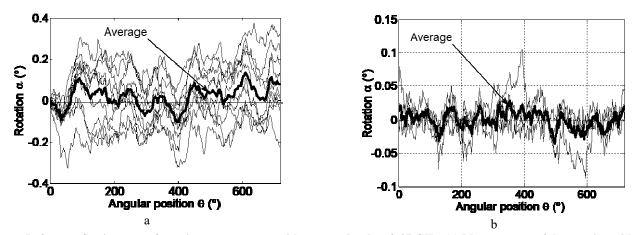

Figure 5. Stray reflections test of rotation measurement without sample when f=27 GHz. (a) Measurement of the rotation without absorbing foams protection (b) Measurement of the rotation when absorbing foams protection are used.
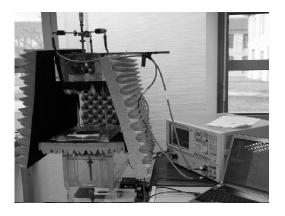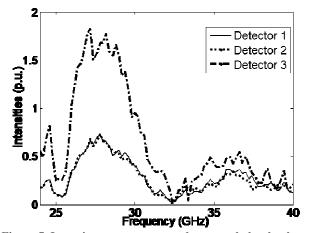

Figure 6. Photo of the experimental bench showing the use of absorbing foams to protect the bench against stray reflection

Figure 7. Intensity spectra measured separately by the three detectors oriented in the incident wave direction
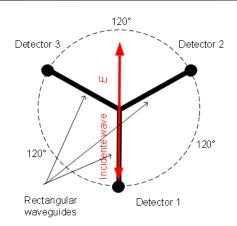
Figure 8. **Positions of detectors with respect to the incident wave direction (reference direction).**
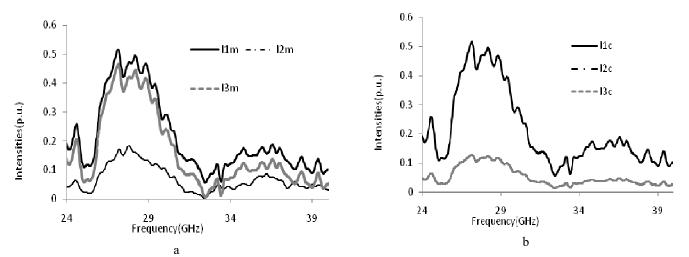

Figure 9. Measured intensity spectra of the three detectors without sample: (a) before calibration (b) after calibration.

- **Systematic errors:** These are due to the imperfections of the whole system. They are time invariant and can be numerically corrected;
- **Random errors:** The internal noise of the components is the main cause. They are random and cannot be easily corrected. However, random errors may be reduced by taking averages of several measurements.

Measurement sensitivity: The relative error of the rotation ($\Delta\alpha/\alpha$) and that of the ellipticity ($\Delta e/e$) are correlated with the noise level of the detectors. Figure (a) and Figure (b) show that averaging several measurements enables the reduction these errors. They also show that the relative error in ellipticity grows more rapidly than the relative error in rotation.

These results may be understood in terms of differential analysis. For any quantity X (I1,I2,I3) which is calculated based on the three intensity measurements, we have:

$$\Delta X/X \approx \Delta(\ln X) \approx \frac{\partial \ln X}{\partial I_1}\Delta I_1 + \frac{\partial \ln X}{\partial I_2}\Delta I_2 + \frac{\partial \ln X}{\partial I_3}\Delta I_3. \tag{17}$$

It is convenient to define

$$\gamma = B/A \quad \text{and} \quad \zeta = \gamma \cos 2\alpha. \tag{18}$$

Then e and α may be expressed in terms of γ and ζ(and conversely) as follows:

$$e = \sqrt{\frac{1-\gamma}{1+\gamma}}; \quad \gamma = \frac{1-e^2}{1+e^2}; \quad \text{and} \quad \alpha = \frac{1}{2} \arccos(\zeta/\gamma).$$

$\Delta e/e$ and $\Delta\alpha/\alpha$ may be expressed in terms of $\Delta\gamma/\gamma$ and $\Delta\zeta/\zeta$:

$$\frac{\Delta e}{e} \approx \frac{d\ln e}{d\gamma}\Delta\gamma = \frac{-1}{2}\left(\frac{1}{1-\gamma}+\frac{1}{1+\gamma}\right)\Delta\gamma = \frac{-\gamma}{1-\gamma^2}\frac{\Delta\gamma}{\gamma} = \frac{e^4-1}{4e^2}\frac{\Delta\gamma}{\gamma}, \tag{19}$$

$$\frac{\Delta\alpha}{\alpha} \approx \frac{\cos 2\alpha}{\alpha\frac{d\cos 2\alpha}{d\alpha}}\frac{\Delta\cos 2\alpha}{\cos 2\alpha} = \frac{-\cot 2\alpha}{2\alpha}\Delta\ln\frac{\zeta}{\gamma} = \frac{\cot 2\alpha}{2\alpha}\left(\frac{\Delta\gamma}{\gamma}-\frac{\Delta\zeta}{\zeta}\right). \tag{20}$$

Now γ and ζ may be re-expressed in terms of I1, I2, I3 as

$$\gamma = \frac{2\sqrt{I_1^2 + I_2^2 + I_3^2 - I_1 I_2 - I_1 I_3 - I_2 I_3}}{I_1 + I_2 + I_3},\tag{21}$$

$$\zeta = \frac{2I_1 - I_2 - I_3}{I_1 + I_2 + I_3}.\tag{22}$$

It follows that

$$\frac{\Delta\gamma}{\gamma} \approx \Delta\ln\gamma = \frac{1}{2}\frac{3\sum_{k=1}^{3}(I_k - A)\Delta I_k}{\sum_{k=1}^{3}I_k^2 - I_1 I_2 - I_1 I_3 - I_2 I_3} - \frac{\sum_{k=1}^{3}\Delta I_k}{\sum_{k=1}^{3}I_k},\tag{23}$$

$$\frac{\Delta\zeta}{\zeta} \approx \Delta\ln\zeta = \frac{2\Delta I_1 - \Delta I_2 - \Delta I_3}{3(I_1 - A)} - \frac{\sum_{k=1}^{3}\Delta I_k}{\sum_{k=1}^{3}I_k},\tag{24}$$

and using the relations

$$3A = I_1 + I_2 + I_3,\tag{25}$$
$$B = A\frac{1-e^2}{1+e^2},\tag{26}$$
And

$$I_1^2 + I_2^2 + I_3^2 - I_1 I_2 - I_1 I_3 - I_2 I_3 = \left(\frac{3}{2}A\gamma\right)^2 = \left(\frac{3}{2}B\right)^2,\tag{27}$$

we obtain finally

$$\frac{\Delta e}{e} \approx \frac{e^4 - 1}{4e^2}\left(\frac{2\sum_{k=1}^{3}(I_k - A)\Delta I_k}{3B^2}, - \frac{\sum_{k=1}^{3}\Delta I_k}{3A}\right)$$

$$\frac{\Delta e}{e} \approx \frac{-(1+e^2)^3}{6A^2 e^2 (1-e^2)}\sum_{k=1}^{3}\left(I_k - A\left(1 + \frac{1}{2}\left(\frac{1-e^2}{1+e^2}\right)^2\right)\right)\Delta I_k,\tag{28}$$

And

$$\frac{\Delta\alpha}{\alpha} \approx \frac{\cot 2\alpha}{6\alpha}\left(\frac{2(1+e^2)^2}{A^2(1-e^2)^2}\sum_{k=1}^{3}(I_k - A)\Delta I_k - \frac{2\Delta I_1 - \Delta I_2 - \Delta I_3}{(I_1 - A)}\right).\tag{29}$$

As $\alpha \to 0$, $\cot 2\alpha = \frac{1}{2\alpha}$ and

$$\frac{\Delta\alpha}{\alpha} \approx \frac{(1+e^2)^2}{3\alpha^2 A^2(1-e^2)^2}\sum_{k=1}^{3}(I_k - A)\Delta I_k - \left(\frac{2\Delta I_1 - \Delta I_2 - \Delta I_3}{12\alpha^2(I_1 - A)}\right).\tag{30}$$

We see in particular that Δe/e and Δα/α become very large as e→0 and α→0 respectively, and in both cases the functional dependence is inverse-square (Δe/e ~ 1/e2 and Δα/α ~ 1/α2 for small e and α, respectively). The relative rotation error depends strongly on the ellipticity, and as ellipticity approaches 1 the relative rotation error becomes very large for all values of α. On the other hand, the ellipticity relative error varies little as α is varied. We also see from (29) that the rotation error can becomes very large if I1≈A (equivalently $I_1 = (I_2 + I_3)/2$).

Measurement noises

In order to understand the origins of the likely measurement errors related to the operation of our experimental device, we carried out several tests without sample. We have proceeded selectively, targeting various parts of the device and evaluating their individual contributions to the overall measurement error.

Vibration effects: A test was performed to determine the influence on measurements (if any) of the vibration caused by the stepper motor. To perform the test, we uncoupled the engine from the cylinder (Figure 1), while leaving the stepper motor on. The source was also left on. Then we took 3600 measurements of the three intensities (Figure 4(a)), and computed the corresponding 3600 estimated rotations using (14). The histogram of the rotation α shows the distribution of the measurements when there is no sample (Figure 4(b)) when the frequency is 29.4 GHz. We also carried out several other tests at frequencies ranging from 24 to 40 GHz. In every case, the distribution followed a normal curve and the magnitude of the rotation error is always within 0.1°. In the particular case shown in Figure 4(b), the standard deviation of the rotation error is 0.48.We conclude that the stepper motor vibration produces negligible noise, which can be reduced even further by averaging the measurements (Michael, 2010).

Effect of stray reflections: The cylinder diameter of our experimental bench is 12 cm. It was experimentally shown in reference [Gambou, 2011] that the diameter of the incident wave beam is 10 cm. Thus using a hollow drum with diameter 12 cm as support for the sample cannot disturb the beam. The effects of vibrations caused by the engine being negligible, the only possible remaining source wave beam are stray reflections. It is known that stray reflections caused by multiple reflections between antennas via the surface of the sample can cause errors [Ghodgaonkar *et al*., 1990]. To perform the test, we first lowered the transmitting horn to the middle of the cylinder, so that the distance between the transmitting and receiving antennas was 30 cm. We then made 10 series of measurements, where in each series the cylinder was rotated from 0 to 720 degrees with no sample. In Figure 5(a), the bold curve represents the averages of the rotation α. Next we moved the emitting antenna to the end of the cylinder, maximizing the distance between the antennas, and placed absorbing foams inside the cylinder and all around the bench in order to limit the stray reflections (Figure 6) We then made 10 more series of measurements as previously. As shown in Figure 5(b) the noise is reduced, indicating that there are fewer stray reflections than in the case of Figure 5(a). The waveforms appear to be completely random and thus not reproducible, but the mean amplitude is very weak (less than 0.1°). We conclude that the rotation error due to stray reflections can be reduced to less than 0.1° through the use of absorbing foams.

Calibration

.Spectrum of measured intensities without sample: Although the three detectors have same manufacture reference number, they were found to have different sensitivities. Figure 7 shows the spectrum of electromagnetic intensities in per unit (p.u.) with no sample when each detector is placed in the incidence direction (OX) which is taken as reference direction. Detector 3 is apparently more sensitive than the other two. Note that these sensitivity measurements may also be influenced by the rectangular waveguide and attenuator.

Calibration procedure: The detector orientations are 120° shifted from each other (Figure 8). We denote by E_1, E_2 and E_3 the electric field amplitude in the direction of detectors 1, 2 and 3respectively. If the detectors are perfectly positioned in the same plane, then when no sample is present the electric field amplitudes are given by the following equations:

$$|E_{20}| = |E_{30}| = |E_{10}\cos(2\pi/3)| = |E_{10}|/2, \tag{31}$$

where the subscript 0 refers to measurement without sample. The corresponding measured electromagnetic intensities are given by

$$I_{10} = |E_{10}|^2, \tag{32}$$

$$I_{20} = I_{30} = |E_{10}|^2/4 = I_{10}/4. \tag{33}$$

However, as shown in Section V.A., the detectors have different sensitivities. That means that

$$I_{20} \neq I_{30} \neq I_{10}/4. \tag{34}$$

Therefore, correction of measured intensities is required. This correction is done numerically through the use of correction coefficients k_2 and k_3 which are determined by the conditions

$$k_2 I_{20} = k_3 I_{30} = I_{10}/4. \tag{35}$$

At any frequency, the coefficients are obtained from measured intensities without sample by the following expressions:

$$k_2(f) = \frac{I_{10}(f)}{4I_{20}(f)}, \tag{36}$$

$$k_3(f) = \frac{I_{10}(f)}{4I_{30}(f)}. \tag{37}$$

Then for any measurement with a sample resulting in intensity values I_1, I_2 and $I_3$for the three detectors respectively, then the corrected intensities should be

$$I_{1c} = I_1, \tag{38}$$

$$I_{2c} = k_2 I_2, \tag{39}$$

$$I_{3c} = k_3 I_3. \tag{40}$$

As an example, Figure 9(a) shows measurements (I1m, I2m, I3m) made without sample with detector 1 in the direction of the incident wave. This figure shows that there is no proportionality of ¼ between the intensity measured by the detector 1 and the two others as expected from (31). But after correction, the proportionality is satisfied (Figure 9(b)).

Conclusion

The experimental bench that we presented has been used to characterize the elliptical polarization of a transmitted wave. In the configuration studied, measurement errors for small rotations and/or small values of the ellipticity are amplified. This implies that the bench is less reliable for measurement of low-loss materials. We have evaluated the influence of the vibration produced by the stepper motor used to rotate the sample. The influence on measurements was shown to be negligible. The use of absorbing foams helps to improve the signal to noise ratio by reducing stray reflections. In the case of our bench, we succeeded in reducing the noise level to under $0.1°$. We have introduced a linear recalibration method to correct for differences in detector sensitivity, and we have demonstrated the accuracy of the correction over a range of frequencies.

REFERENCES

Alkanoo, A. A., Taya S. A. and El-Agez, T. M. 2015. "Effect of the orientation of the fixed analyzer on the ellipsometric parameters in rotating polarizer and compensator ellipsometer with speed ratio 1:1," Opt Quant Electron, vol. 47, no. 7, p. 2039–2053.

Aspnes, D. E. 1973. "Fourier transform detection system for rotating analyzer ellipsometer," Opt. Commun, vol. 8, no. 3, pp. 222-225.

Azzam and M. Bashara, 1996. Ellipsometry and polarized light, Amsterdam: North Holland: Elsevier Science B. V.

Azzam R. and Bashara, N. 1977. Ellipsometry and polarized light, North-Holland, Amsterdam.

Azzam R. and Bashara, N. 1987. Light, Ellipsometry and polarized, Amsterdam: Elsevier science.

Azzam, R. 1975. "Polar curves for transmission ellipsometry," Optics communications, vol. 14, no. 1, pp. 145-147.

El-Agez, T., Taya S. and Tayyan, A. 2010. A polynomial approach for reflection, transmission, and ellipsometric parameters by isotropic stratified media," Opt Appl, vol. 40, p. 501–510.

Gambou, F. 2009. "Ellipsometry on a planar S-shape material," Progress In Electromagnetics Research Letters, vol. 9, p. 1–8.

Gambou, F., Bayard B. and Noyel, G. 2011. "Characterization of material anisotropy using microwave ellipsometry," Microwave and optical technology letters, vol. 53, no. 9, pp. 1996-1998, September.

Ghodgaonkar, D., Varadan V. and Varadan, V. 1990. "Free-space measurement of complex permittivity and complex permeability of magnetic materials at microwave frequencies," *Instrumentation and Measurement IEEE Transactions*, vol. 39, no. 2, p. 387 – 394.

González, A. G., Herrado M. Á. and Asuero, A. G. 2010. "Intra-laboratory assessment of method accuracy (trueness and precision) by using validation standards," Talanta, vol. 82, no. 5, p. 1995–1998.

Jarosik, N., Bennett, C. L., Dunkley, J., Gold, B., Greason, M. R., Halpern, M., Hill, R. S., Hinshaw, G., Kogut, A., Komatsu, E., Larson, D., Limon, M., Meyer, S. S., Nolta, M. R., Odegard, N., Page, L., Smith, K. M., Spergel D. N. and Tucker, G. S. 2011. "Seven-year WILKINSON Microwave Anisotropy Probe (WMAP) observations: sky maps, systematic errors, and basic results," Astrophysical Journal Supplement Series, vol. 192, no. 2.

Michael, K. 2010. Errors of measurement, Theory, and Public policy, New Jersey: Educational Testing Service.

Moffat, R. J. 1988. "Describing the uncertainties in experimental results," *Experimental Thermal and Fluid Science*, vol. 1, no. 1, p. 3–17.

Moungache, A., Bayard, B., Tahir, A. M., Robert, S., Gambou F. and Jamon, D. 2013. "Microwave oblique transmission ellipsometric method for measurement of thick and non-transparent materials," *Revue Scientifique du* CNAR, vol. 1, no. 2, pp. 38-43.

Moungache, A., Bayard, B., Tahir, A. M., Robert, S., Jamon D. and Gambou, F. 2015. "Measurement of refraction index of thick and nontransparent isotropic material using transmission microwave ellipsometry," Microwave and Optical Technology Letters, vol. 57, no. 4, p. 1006–1013, April.

Oates, T., Ryves L. and Bilek, M. 2008. "Dielectric functions of a growing silver film determined using dynamic in situ spectroscopic ellipsometry," Opt Express, vol. 16, p. 2302–2314.

Raoult, G. 1958. Les ondes centimetriques, Paris: Masson.

Sagnard, F., Seetharamdoo D. and Glaunec, V. L. 2002. "Reflection and transmission ellipsometry data analysis for measuring complex permittivity fo single-layer material at microwave frequencies," *Microwave and Optical Technology Letters*, vol. 33, no. 6, pp. 444-448, June 20.

Taya S. A. and El-Agez, T. M. 2013. "Rotating polarizer analyzer ellipsometer with a fixed compensator," Optik 124, pp. 3379-3383.

Taya, S. A., El-Agez T. M. and Alkanoo, A. A. 2014. "A spectroscopic ellipsometer using rotating polarizer and analyzer at a speed ratio 1:1 and a compensator," *Opt Quant Electron*, vol. 46, pp. 883-895.

Taylor and J.R. 1982. An Introduction to Error Analysis: *The Study of uncertainties in Physical Measurement,* Mill Valley: CA: University Science Books.

Wehus, U. Fuskeland and H. K. Eriksen, 2013. "The effect of systematics on polarized spectral indices," *Astrophysical Journal Supplement Series*, vol. 763, no. 2, pp. 763-138.

****